Asian Journal of Chemistry; Vol. 38, No. 9 (2026), 2398-2408
ASIAN JOURNAL OF CHEMISTRY
https://doi.org/10.14233/ajchem.2026.36509

Theoretical Analysis of Multimetal Complexation of Pr(III):L-leucine:Mg(II): Thermo-Kinetic Studies of the Reaction Pathways

ZEVIVONÜ THAKRO, MHASIRIEKHO ZIEKHRÜ, SHEPAZO CHIZO and M. INDIRA DEVI*

Department of Chemistry, Nagaland University, Lumami-798627, India

*Corresponding author: E-mail: indira@nagalanduniversity.ac.in

Received: 25 May 2026 *Accepted*: 7 August 2026 *Published online*: 5 September 2026 AJC-22467

The 4*f*-4*f* absorption spectra of Pr^{3+} were employed as sensitive probes to investigate the interaction of Pr^{3+} with L-leucine in the presence and absence of Mg^{2+} in various aquated organic solvents, namely DMF, acetonitrile (ACN), dioxane and methanol. The interaction of Pr^{3+} with L-leucine was evaluated through the determination of spectroscopic energy parameters, including the Slater-Condon parameters (F_k), spin-orbit coupling parameter (ξ_{4f}), bonding parameter ($b^{1/2}$), nephelauxetic ratio (β), percentage covalency (δ) and Racah parameter (E^k). These parameters were used to assess changes in the electronic environment and the nature of metal–ligand interactions. Variations in the absorption intensity parameters, including the oscillator strengths (P) of the individual 4*f*-4*f* transitions and Judd-Ofelt intensity parameters (T_λ), provided further evidence for the coordination of L-leucine with Pr^{3+}. Upon addition of L-leucine, the characteristic absorption bands of Pr^{3+} exhibited bathochromic shifts accompanied by hyperchromic effects, which confirmed the changes in the coordination environment and electronic structure of the metal ion. The influence of Mg^{2+} on the Pr^{3+}–L-leucine interaction was further examined to elucidate its role in the complexation process. Kinetic and thermodynamic investigations were subsequently performed to determine the mechanism, stability and energetics of complex formation in the different solvent systems. The combined spectroscopic, kinetic and thermodynamic results provide insight into the nature of Pr^{3+}–L-leucine interactions and the influence of Mg^{2+} and solvent environment on their complexation behaviour.

Keywords: Oscillator strength, Pseudohypersensitive, Thermodynamics, L-leucine, Lanthanide.

INTRODUCTION

The 4*f*-electron based lanthanide binary compounds have piqued interest in the last few decades from both a fundamental and an applied standpoint [1,2]. Numerous experimental and theoretical studies were carried out to better understand the role of *f*-electrons in this area [3,4]. Lanthanides are predominantly in their +3 oxidation state in aqueous media, although there are other oxidation states accessible, under normal conditions lanthanides are predominantly in their +3 state [5-7]. A growing number of biomolecular reactions using lanthanides to investigate their structural functions have sparked interest in the coordination chemistry of lanthanides in solution. This results mainly from their resemblance and capability to replace calcium ions [8-10]. Lanthanide biochemistry is largely influenced by their 4*f*-electrons. Hence, the 4*f*-electrons serve as a weak barrier against rising nuclear charge for the outer shells since 4*f*-orbitals have a radial probability distribution nearer to the nucleus as compared to 5*p*- and 6*s*-electrons [11].

It is familiar that amino acids carry out a wide range of biological functions and play an important role in biological systems. Leucine (2-amino-4-methylpentanoic acid), an amino acid, functions as a substrate for protein synthesis and thus is crucial for modulating protein metabolism [12]. The carbon skeleton of leucine can also be used to produce ATP, just like that of other amino acids. The effects of leucine supplementation have been studied in a variety of conditions, including aging, muscle injury, obesity, protein/ energy deficiency and diabetes mellitus [13,14]. The prevalence of metabolic illnesses has increased to alarming levels around the world and since leucine modulates signaling pathways involved in metabolism regulation, researching nutritional supplements containing leucine that may be useful in the treatment and prevention of obesity and diabetes has become critical [15,16]. Though L-leucine plays a key function in human metabolism, its balance is crucial; too little can cause pellagra leucine, while too much can induce low blood sugar (hypoglycemia) [17]. Physiologically, peptides and amino acids can act as

effective metal binding sites. Peptides are considered the simple building blocks of amino acids. In addition to their biological importance, peptides are among the most actively researched molecules today due to their medicinal properties [18,19]. An investigation of the interaction of metals and ligands using a probe to detect 4*f*-4*f* spectra of Pr^{3+} would therefore be an exciting opportunity to study in depth.

Magnesium (Mg) is an essential mineral in the human body and plays a central role in the regulation of numerous physiological processes. It functions as a cofactor or activator in more than 300 enzymatic reactions and is involved in RNA and DNA synthesis, protein, lipid and carbohydrate metabolism, maintenance of cell membrane stability, bone formation and calcium homeostasis, as well as the proper functioning of the nervous and immune systems [20-22]. Despite its important biological role, Mg(II) is spectroscopically less amenable to direct investigation because of its closed-shell electronic configuration and diamagnetic nature. Lanthanide(III) ions, in contrast, possess characteristic and highly sensitive 4*f*-4*f* transitions that can serve as useful spectroscopic probes. Therefore, substitution of Mg^{2+} with a Ln(III) ion, such as Pr(III), provides an indirect spectroscopic approach for gaining deeper insight into metal–amino acid interactions and the coordination behaviour of amino acids relevant to biological systems.

In this work, 4*f*-4*f* spectra of Pr^{3+} was used as spectral and structural tool to investigate the reaction when Pr(III) ion interacts with L-leucine [Pr(III):Leu] with or without Mg^{2+} in the mixture of water and organic solvents. The ratio of the aquated organic solvents (CH_3CN, CH_3OH, $C_4H_8O_2$ and DMF) was 50%v/v. Differences in the theoretically calculated values of the following parameters: bonding parameters ($b^{1/2}$), percentage covalency (δ), nephelauxetic ratio (β), Slater-Condon (F_k), Racah energy (E_k) and spin-orbit interaction (ξ_{4f}) were employed to look into the insight of the complexation. To explore the various 4*f*-4*f* transitions under varied conditions, the intensity parameters, Judd-Ofelt T_λ (λ = 2, 4, 6) and oscillator strengths (P) were determined. An investigation of the reaction dynamics of Pr^{3+} with L-leucine and Mg^{2+} in different temperatures and time conditions, could provide a systematic analysis of the nature of chemical reactions along with the thermodynamic behaviour by evaluating variables such as rate constant (k), frequency/pre-exponential factor (A), ΔH^o, ΔS^o and ΔG^o.

EXPERIMENTAL

$Pr(III)(NO_3)_3{\cdot}6H_2O$ (99.9%) was acquired from Sigma-Aldrich, 2-Amino-4-methylpentanoic acid (L-leucine extra CHR, 99%) from HiMedia and the solvents (1,4-dioxane, acetonitrile, N,N-dimethylformamide, methanol) were all procured from Merck (99.5% assay). A concentration of 5×10^{-3} M for Pr(III), L-leucine and magnesium ion (+2) was maintained for the absorption study. Four different aquated organic solvents (50% vol./vol.) [dioxane, acetonitrile (ACN), methanol (MeOH) and dimethylformamide (DMF)] were used in all the preparations. The UV/Vis spectrophotometer (Perkin Elmer Lambda 365) was used to record the absorption spectra.

Lanthanide(III) complexes of amino acids: The functional groups, –COOH and $–NH_2$ are present in amino acids and they have the capability to adjust the dimensions as well as magnitude of favourable substance, in order to carry on the integrity of its -R group [23]. L-Leucine exist in a state of neutrality in gaseous phase [24] and as zwitterions in aqueous solution [25-27]. The pH values affect how the ligand bonds to the metal; for example, in acidic medium, only the oxygen atom attaches to the metal, while in basic medium, nitrogen and oxygen atoms are both bonded to the metal as shown in Fig. 1 [28].

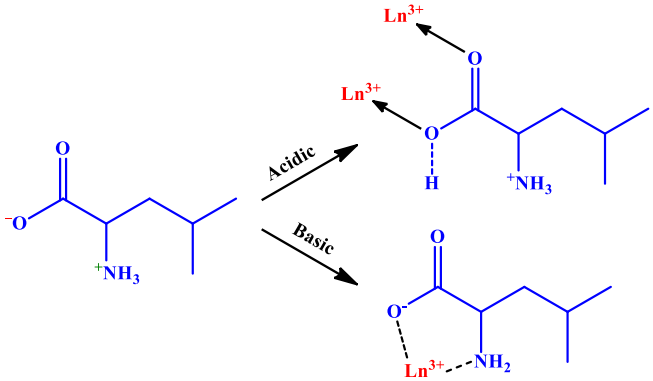

Fig. 1. Bonding properties of L-leucine at various pH medium

When it comes to complex formation, lanthanides are regarded as hard acceptors or class A and thus favour hard acceptor or class A ligands (in the order Cl < F < S < N < O). Coordination numbers are typically between six and twelve, but biologically relevant coordination numbers are eight or nine. This results in the complexes being capable of various geometrical configurations [29]. The possible nona-coordinated complex of Pr(III) and L-Leucine is shown in Fig. 2.

Computation

Energy parameters: The formation of the complex of the metal with ligand is measured by the Nephelauxetic ratio, which serves as a covalency indicator. In order to explain the nephelauxetic effect, the Slater-Condon and Racah parameters have been interpreted as follows:

$$\beta = \frac{F_k^C}{F_k^f} \text{ or } \frac{E_k^C}{E_k^f} \quad (1)$$

where Racah parameters are given as E_k which is related to the complex formed and pure metal while Slater-Condon variable refers F^k (k = 2, 4, 6).

The β-effect is associated with bonding parameter and is measured as the extend of 4*f*-orbital mingle. The covalent percentage and bonding variable can be evaluated with the following relations:

$$b^{1/2} = \left(\frac{1-\beta}{2}\right)^{1/2} \quad (2)$$

$$\delta = \left(\frac{1-\beta}{\beta}\right) \times 100 \quad (3)$$

As the electrostatic interchange and the spin-orbit interchange between 4*f*-electrons make up the energy (E_{so}) of the 4*f*-electron transformation, these may be described as:

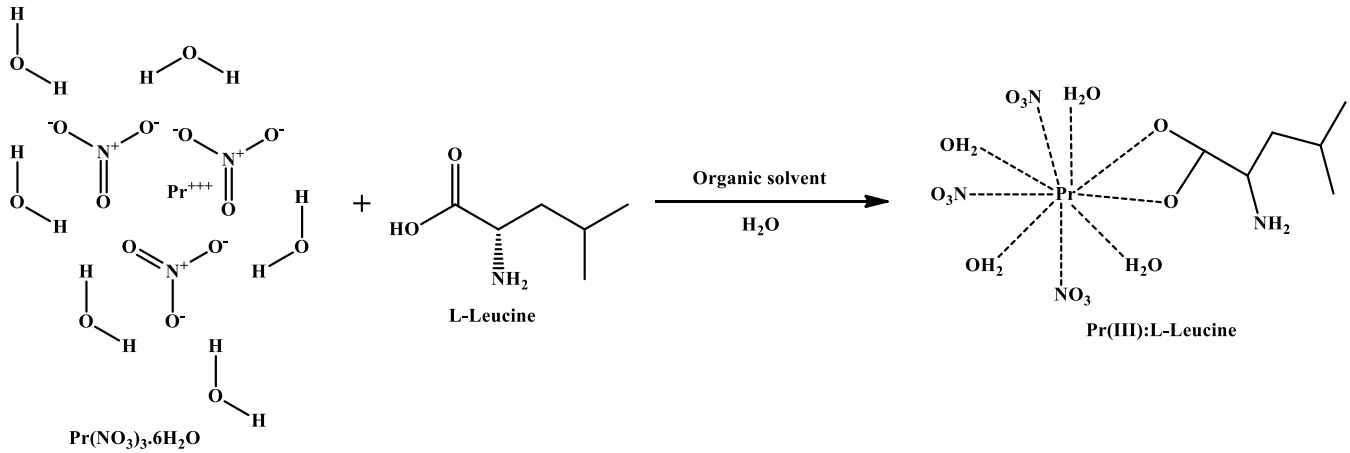

Fig. 2. Possible interaction between Pr^{3+} and L-leucine in acidic media

$$E_{so} = A_{so}\ \xi_{4f} \quad (4)$$

where radial integral is represented by Lande's parameter 'ξ_{4f}' and an angular interaction is indicated by 'A_{so}'.

To calculate the energy level of the $4f^n$ arrangement, radial integrals such as F_2, F_4, F_6 and ξ_{4f} are needed. Energy at the j^{th} level can be obtained as:

$$E_j(F_k, \xi_{4f}) = E_{oj}(F_k^o, \xi_{4f}^o) + \frac{\partial E_j}{\partial \xi_{4f}} \Delta\xi_{4f} \quad (5)$$

Here, the initial energy 'E_{0j}' is the zero-order energy of the j^{th} level. Following are some equations representing equated used of F_k and ξ_{4f}.

$$F_k = F_k^o + \Delta F_k \quad (6)$$

$$\xi_{4f} = \xi_{4f}^o + \Delta\xi_{4f} \quad (7)$$

The value of ΔE_j is calculated as the distinction between E_j and E_{0j} values given as:

$$\Delta E_j = \Sigma_{k,2,4,6} \frac{\partial E_j}{\partial F_k} + \frac{\partial E_j}{\partial \xi_{4f}} \Delta\xi_{4f} \quad (8)$$

Solving the above equation by utilizing the least square method will provide the value of ΔF_2 and $\Delta\xi_{4f}$. The approximate value of F_4 and F_6 can be calculated by using the formula given below:

$$\frac{F_4}{F_2} = 0.1380 \text{ and } \frac{F_6}{F_2} = 0.0150 \quad (9)$$

Oscillator strength (P): The intensity of the absorption band is measured by the oscillator strength (P), which is directly related to the dimension of absorption curve. Relationship between the energy of transitional wavenumber (ν), the molar extinction coefficient (ε_{max}) and the refractive index (η) of the medium can be used to obtain the oscillator strength (P) as:

$$P = 4.6\times10^{-9}\left(\frac{9\eta}{(\eta^2+\eta)^2}\right)\int \varepsilon_{max}\,\bar{\nu}\,d\bar{\nu} \quad (10)$$

Molar extinction, wave number and refractive index coefficient are each represented by the symbols, ε_{max}, $\bar{\nu}$ and η, respectively.

From the absorption band, we can determine the experimental oscillator strength (P_{obs}) values by employing the Gaussian curve analysis as:

$$P_{obs} = 4.6\times10^{-9}\times\varepsilon_{max}\,\bar{\nu}_{1/2} \quad (11)$$

$\bar{\nu}_{1/2}$ = Half bandwidth [30-32].

Judd-Ofelt parameters (T_λ): The aquo ions of lanthanides were subsequently incorporated into the computation of the oscillator strengths [32]. Using least-squares fitting and alternative numerical methods commonly employed in solution spectral research, as given below:

$$P = \chi\left(\frac{8\pi^2 mc}{3h}\right)\sigma\Sigma T_\lambda \,\|\, U^{(\lambda\lambda)} \,\|\, (2J+1) \quad (12)$$

Through the matrix of the unit tensor operator ($U^{(\lambda)}$) of rank λ, the T_λ phenomenological variables keep both the ground and final state ($<f^n\Psi J|$ & $|f^n\Psi' J'|$, respectively) connected [33]. These quantities exhibit a sensitive nature toward the type of the transition employed in its computations and the degree of precision of oscillator strength [34].

Based on the Judd and Ofelt's theoretical of band intensities, an empirical approach was used in the theoretical calculation [32-36]. The transition character is considered to be an essentially that of an electric dipole, while the oscillator strength corresponds with the induced electric dipole transition $\Psi J \rightarrow \Psi' J'$, which is shown below by the equation given [37,38]:

$$P = \Sigma_{\lambda=2,4,6} T_\lambda \sigma(f^N \Psi J \,\|\, U^\lambda \,\|\, f^N \Psi' J')^2 \quad (13)$$

In this case, '$U^{(\lambda)}$' stands for the matrix element. T_2, T_4 and T_6 are the three quantities associated with the radial parts of the $4f^N$ wave functions.

With respect to the absorption of the radiant energy, the following equation represents the correlation between the observed intensity of the absorption band and the probability (P).

$$P = \frac{2.303mc^2}{N\pi e^2}\int \varepsilon_i(\sigma)\,d\sigma$$

or,

$$P = 4.314\times10^{-9}\int \varepsilon_i(\sigma)\,d\sigma \quad (14)$$

Using the remark oscillator strength (P_{obs}) of the lanthanide, Judd and Ofelt calculated the lanthanide intensity as follows:

$$\frac{P_{obs}}{\nu} = [U^2]^{2-}T_2 + [U^2]^2.T_4 + [U^2]^2.T_6 \quad (15)$$

where, ν = wavenumber and U = matrix element.

Any indication of a relationship between the nephelauxetic band shift and the structure is very important in spectral studies of the structural properties of lanthanide coordination compounds in solution. The correlation between the coordination number and the nephelauxetic effect was observed by Jorgensen & Ryan [39], which indicate that a drop in the coordination number causes a decrease in the metal-ligand distance. In order to clarify the correlation, assessments of the interactions between the nephelauxetic effect, geometry and energy factors have been carried out. According to the angular overlap model, "n" has a direct relationship to the nephelauxetic effect and can be expressed as:

$$n = \left(\frac{(1-\beta^{1/2})}{\beta^{1/2}}\right) \quad (16)$$

$$n = \left(\frac{H^2L}{(H_M - H_L)^2}\right)(S*R)^2N \quad (17)$$

where N is the coordination number, HM and HL are coulomb integrals of the atomic orbital, S is the overlap integral and R is the radius of the orbit. For compounds with ligands coordinated by identical donor atoms, the first term on the RHS of eqn. 17 is a constant, which becomes:

$$n = \text{Constant}\ (S*R)^2N \quad (18)$$

Eqn. 18 demonstrates the nephelauxetic effect with two variables. Nonetheless, any fluctuation in the value of R results in a more significant alteration in $(S*R)^2$ than in N. S*R and N display fluctuations, which are inversely related to changes in the lanthanide–ligand distance.

Underlying principles of thermo-kinetics: Activation energy of a complex was calculated employing Arrhenius reaction rate equation by plotting log k (k = rate constant) *versus* 1/T.

$$\log k = \log A - \frac{E_a}{2.303R}\frac{1}{T} \quad (19)$$

Pre-exponential factor "A" in this context refers to the orientation or frequency likelihood of collisions. The slope is employed to evaluate the activation energy, which is then provided by:

$$E_a = -\text{Slope} \times 2.303 \times R \quad (20)$$

By determining the activation energy (E_a), the reaction rate (k) was determined.

The thermos-kinetics variables for the complexation have been evaluated by van't Hoff plot of log k *versus* $1/T \times 10^3$ shown below:

$$\log k = -\frac{\Delta H^o}{R}\left(\frac{1}{T}\right) + \frac{\Delta S^o}{R} \quad (21)$$

In comparison to the frequency factor "A", the specific rate constant "k" increases in a noticeable and significant way as the temperature "T" rises. As a result, under such condition "A" is neglected.

RESULTS AND DISCUSSION

It has been proven that utilization of absorption spectrophotometry, in the chemistry of lanthanides, particularly in solutions can provide an insight into complexes with intricate *f*-electron transitions and sensitivity of lanthanide to the complex's shape and coordination environment, has made it a viable tool for investigating the chemistry of lanthanides [40-42]. The strength of the metal-ligand bond, coordination geometry, shape of the complex produced and interaction of chelate-solvent can be determined by 4*f*-4*f* absorption spectra of lanthanide ions [30].

The hypersensitive transitions show a high level of sensitivity when their coordination environment is changed. They adhere to the selection rules, $\Delta S = 0$, $\Delta L \leq 2$ and $\Delta J = \leq 2$, so as the metal ion complexes with the ligands, their band intensities increase [43]. The 4*f*-4*f* transitions are located deep inside the metal's core-shell and they are often not affected by the variation in its coordination environment, therefore make them a non-hypersensitive transition [44].

Studies have shown that several Pr^{3+} transition intensities do not adhere to the selection rule, but they can still be very delicate to minor variations in their coordinating domain adjacent to them. Such transitions, are commonly referred to as ligand mediated pseudohypersensitive transitions ($^3H_4 \rightarrow {}^3P_2$, $^3H_4 \rightarrow {}^3P_1$, $^3H_4 \rightarrow {}^3P_0$ and $^3H_4 \rightarrow {}^1D_2$) [45-47]. A large number of absorption studies have been employed for better understanding of pseudohypersensitive transitions of the ligand and Pr^{3+} interactions, as well as their structural conformations in solution [8,18]. The increase intensity of the pseudo hypersensitive transitions vividly demonstrates the possibility of Pr^{3+}-ligand interaction and the effect of their sensitivity on complex formation.

Under different experimental conditions, the P and T_λ parameters for the pseudohypersensitive transitions of free Pr^{3+} and Pr^{3+} complex with L-leucine and Mg^{2+} is shown in Table-1.

According to the P values of the 4*f*-4*f* bands in Table-1, the remarkable variation in the P value suggest the possibility of Pr^{3+} interacting with L-leucine [48]. Pr^{3+} interacting with the ligand causes the amplitude of T_λ ($\lambda = 2, 4, 6$) parameters increases immensely; this validates the ability of L-leucine to bind to Pr^{3+}. The intensity was further increased by adding Mg^{2+} to the Pr(III):Leu complex. This could be due to its ability to bind with Mg^{2+} to produce a multimetal complex [23]. The assessed T_4 and T_6 values vary greatly; its values are found to be positive, thereby they can be utilized in the Judd-Ofelt theory of 4*f*-4*f* transitions. The symmetry characteristics of the complex species are related to changes in both the T_4 and T_6 parameters [49]. As a result, significant variations in T_4 and T_6 values indicate that their immediate coordination domain has changed, thus resulting in changes in Pr^{3+} complexation with ligands. In contrast T_2 is ignored as it is connected to the hypersensitive transition, $^3H_4 \rightarrow {}^3F_3$, which is outside of the UV-Visible region and has negative values [42]. A major change in P and its corresponding T_λ

TABLE-1
OBSERVED AND CALCULATED P AND T_λ (λ = 2, 4, 6) cm^{-2} INTENSITY PARAMETER OF Pr(III) WITH L-LEUCINE IN PRESENCE AND ABSENT OF Mg^{2+} IN DIFFERENT AQUATED ORGANIC SOLVENT

System	$^3H_4 \rightarrow {}^3P_2$		$^3H_4 \rightarrow {}^3P_1$		$^3H_4 \rightarrow {}^3P_0$		$^3H_4 \rightarrow {}^1D_2$		T_2	T_4	T_6
	P_{obs}	P_{cal}	P_{obs}	P_{cal}	P_{obs}	P_{cal}	P_{obs}	P_{cal}			
DMF:Water											
Pr(III)	5.355	5.355	1.826	1.288	0.739	1.270	0.915	0.915	-147.4	3.54	16.61
Pr(III):Leu	7.838	7.838	2.991	2.038	1.071	2.010	1.125	1.125	-265.5	5.61	24.24
Pr(III):Leu:Mg(II)	8.803	8.803	3.884	2.780	1.651	2.738	1.548	1.548	-235.4	7.66	26.91
ACN:Water											
Pr(III)	4.348	4.348	1.726	1.289	0.837	1.267	0.967	0.967	-70.03	3.53	13.32
Pr(III):Leu	6.770	6.770	2.353	1.827	1.280	1.797	1.132	1.133	-193.5	5.01	20.88
Pr(III):Leu:Mg(II)	8.361	8.3618	3.067	2.202	1.315	2.166	1.789	1.789	-150.0	6.05	25.86
Dioxane:Water											
Pr(III)	3.710	3.715	1.122	0.841	0.549	0.825	0.020	0.020	-241.5	2.30	11.55
Pr(III):Leu	5.869	5.869	1.761	1.341	0.905	1.317	0.429	0.429	-291.8	3.67	18.25
Pr(III):Leu:Mg(II)	6.894	6.894	2.737	1.646	0.546	1.619	0.781	0.782	-280.5	4.52	21.43
Methanol:Water											
Pr(III)	3.468	3.468	1.489	0.852	0.211	0.838	1.202	1.202	-283.6	2.33	10.74
Pr(III):Leu	4.309	4.309	1.587	1.094	0.591	1.077	1.342	1.342	18.2	3.00	13.33
Pr(III):Leu:Mg(II)	5.120	5.120	2.615	1.767	0.905	1.739	1.885	1.885	86.3	4.85	15.51

value represents the inner-sphere coordination, on the other hand a small change in these values denotes outer-sphere coordination [43]. Alterations in the values of P and T_λ support the involvement of L-leucine in the inner-sphere complexation of Pr^{3+}. The evaluated parameters identify T_6 as the most sensitive parameter for describing the interaction of L-leucine with Pr^{3+} in the presence of Mg^{2+}, followed by T_4 and T_2, with the sensitivity order $T_6 > T_4 > T_2$.

Evaluated values of the energy interaction variables F_k (k = 2, 4, 6), ξ_{4f}, E_k (k = 1, 2, 3), β, $b^{1/2}$ and δ are shown in Table-2. The energy of 4*f*-4*f* bands alter distinctly which may be due the binding of Pr(III)–L-leucine. A clear speculation of the bonding nature could be predicted from the changes of the various evaluated parameters shown in Table-2. The bonding characteristics of Pr^{3+} in Pr(III):Leu and Pr(III):Leu:Mg(II) complexes in aquated organic solvents (ACN, DMF, dioxane and methanol) can be assessed from changes in the energy interaction parameters. Comparison of these parameters with those of free Pr^{3+} shows a decrease in the Slater-Condon parameters (F_k) and interelectronic repulsion parameters, particularly ξ_{4f} and β. These changes are consistent with the nephelauxetic effect associated with complex formation and indicate modification of the electronic environment around Pr^{3+} upon coordination with L-leucine.

Table-2 shows that the energy interaction parameters decrease appreciably upon complexation, which may be associated with expansion of the central metal-ion orbital and a consequent reduction in the metal–ligand bond distance. This interpretation is consistent with the observed changes in the *f-f* transition intensities. The nephelauxetic ratio (β) for Pr^{3+} in the presence of L-leucine remains below unity, supporting a degree of covalent character in the Pr(III)–L-leucine inter-

TABLE-2
COMPUTED VALUE OF SLATER-CONDON F_k (cm^{-1}), LANDE ξ_{4f} (cm^{-1}), RACAH E^k (cm^{-1}), NEPHELAUXETIC EFFECT (β), BONDING ($b^{1/2}$), COVALENCY (δ) AND ROOT MEAN SQUARE (RMS) VALUES OF THE DIFFERENT Pr(III) SYSTEMS

System	F_2	F_4	F_6	ξ_{4f}	E^1	E^2	E^3	β	$b^{1/2}$	δ	RMS
DMF:Water											
Pr(III)	308.895	42.643	4.664	719.965	3507.395	23.735	614.104	0.944	0.166	5.856	122.50
Pr(III):Leu	308.592	42.601	4.659	719.767	3503.955	23.712	613.502	0.943	0.167	5.921	121.20
Pr(III):Leu:Mg(II)	308.112	42.535	4.653	719.934	3498.504	23.675	612.547	0.942	0.168	5.987	123.16
ACN:Water											
Pr(III)	309.209	42.686	4.669	722.420	3510.959	23.759	614.728	0.946	0.163	5.617	111.79
Pr(III):Leu	308.957	42.651	4.665	722.256	3508.109	23.740	614.229	0.944	0.164	5.670	110.64
Pr(III):Leu:Mg(II)	308.602	42.602	4.659	721.918	3504.068	23.713	613.521	0.943	0.166	5.754	113.70
Dioxane:Water											
Pr(III)	309.466	42.721	4.672	724.099	3513.879	23.779	615.2392	0.948	0.1607	5.447	108.47
Pr(III):Leu	309.157	42.679	4.668	723.446	3510.373	23.755	614.6254	0.947	0.1621	5.547	113.65
Pr(III):Leu:Mg(II)	308.794	42.629	4.662	721.657	3506.251	23.727	613.9036	0.945	0.1648	5.743	118.97
Methanol:Water											
Pr(III)	309.419	42.715	4.672	721.556	3513.344	23.775	615.145	0.947	0.163	5.649	113.30
Pr(III):Leu	309.213	42.686	4.669	720.995	3511.006	23.759	614.736	0.945	0.164	5.725	114.65
Pr(III):Leu:Mg(II)	308.955	42.651	4.665	720.444	3508.078	23.739	614.223	0.944	0.167	5.810	120.55

action [44]. The progressive decrease in β may arise from expansion of the 4*f*-orbital and increased metal–ligand orbital overlap, leading to a shorter effective bond distance [50-52]. The decrease in β is accompanied by enhanced intensities of the Pr^{3+} transitions, particularly $^3H_4 \rightarrow {}^3P_2$, $^3H_4 \rightarrow {}^3P_1$, $^3H_4 \rightarrow {}^3P_0$ and $^3H_4 \rightarrow {}^1D_2$). Energy interaction parameters precision is estimated using root mean square (RMS) values.

The data presented in Tables 1 and 2 provide insight into the solvent-dependent complexation of Pr^{3+} with L-leucine. Variations in the oscillator strengths (P) and Judd-Ofelt intensity parameters (T_λ) for the 4*f*-4*f* transitions reflect changes in the interaction between the Pr^{3+} 4*f*-orbitals and ligand orbitals. The highest values of P and T_λ were obtained in DMF, which indicate a stronger influence of this solvent on complex formation. The larger oscillator strengths observed in DMF, compared with ACN, dioxane, and methanol, point to a higher preference for complex formation in this medium [53,54]. The higher values of the bonding parameter ($b_{1/2}$) and percentage covalency (δ) in DMF further support enhanced metal–ligand covalent character, which may be associated with the presence of the donor nitrogen atom of L-leucine [20]. The solvent sensitivity follows the order: DMF > CH_3CN > $C_4H_8O_2$ > CH_3OH.

The four pseudo-hypersensitive transitions and their corresponding absorption spectra for free Pr^{3+} and the complexes formed in dioxane and DMF are shown in Figs. 3 and 4. The 4*f*-4*f* transitions of Pr^{3+} are highly sensitive to changes in the local coordination environment. Addition of L-leucine to the Pr^{3+} solution resulted in increased absorption intensity and bathochromic shifts of the characteristic bands. Subsequent addition of Mg^{2+} produced a further increase in band intensity that indicate the changes in the coordination environment of Pr^{3+} upon formation of the Pr(III):Leu(II) system [44,48,49].

The kinetics of Pr(III):Leu(II) complex formation was investigated in 50% (v/v) DMF-H_2O at different temperatures. Absorption spectra were recorded at 303, 308, 313 and 318 K over selected time intervals. The corresponding spectra are

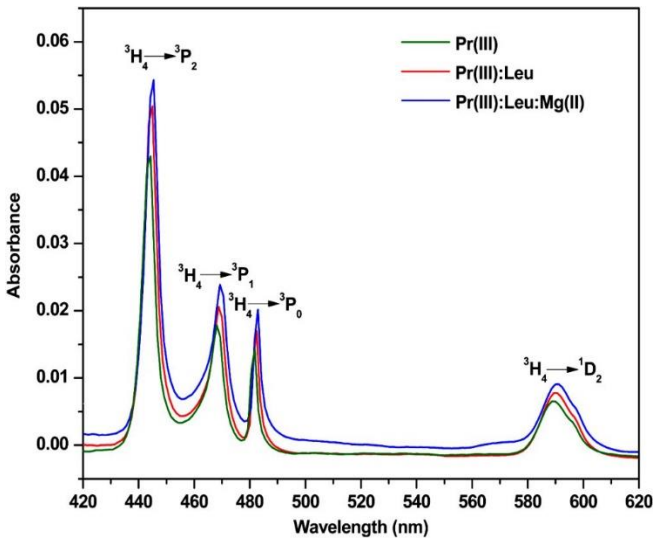

Fig. 3. 4*f*-4*f* electronic transition absorption spectra (UV-vis) of Pr^{3+}, Pr(III):Leu & Pr(III):Leu:Mg(II) complex in dioxane mixed with water (50% v/v)

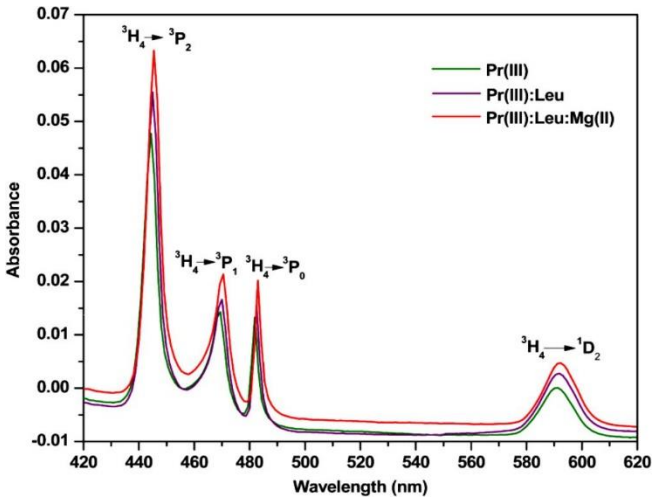

Fig. 4. 4*f*-4*f* electronic transition absorption spectra (UV-vis) of Pr^{3+}, Pr(III):Leu & Pr(III):Leu:Mg(II) complex in DMF mixed with water (50% v/v)

shown in Figs. 5 and 6, while the calculated P and T_λ values are compiled in Tables 3-6. Among the investigated 4*f*-4*f*

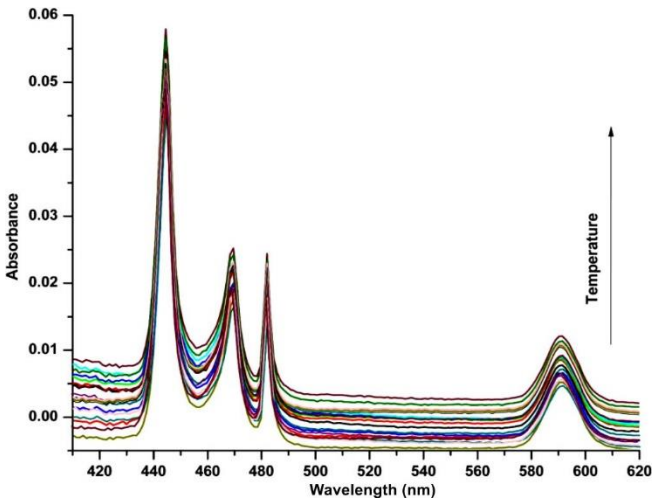

Fig. 5. Absorption spectra of Pr(III):Leu:Mg(II) complexation at 298 K and in different time intervals

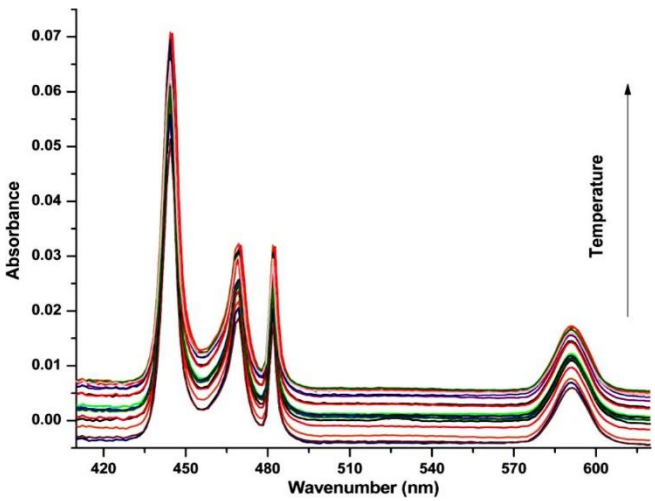

Fig. 6. Absorption spectra of Pr(III):Leu:Mg(II) complexation at 303 K and in different time intervals

TABLE-3
OBSERVED AND CALCULATED P AND T_λ, (λ = 2, 4, 6) cm^{-2} AT 298 K AND IN VARIOUS TIME INTERVALS FOR THE COMPLEX Pr(III):Leu:Mg(II)

Time	$^3H_4 \rightarrow {}^3P_2$		$^3H_4 \rightarrow {}^3P_1$		$^3H_4 \rightarrow {}^3P_0$		$^3H_4 \rightarrow {}^1D_2$		T_2	T_4	T_6
	P_{obs}	P_{cal}	P_{obs}	P_{cal}	P_{obs}	P_{cal}	P_{obs}	P_{cal}			
0	5.068	5.068	1.638	1.229	0.808	1.212	0.969	0.969	-116.2	3.37	15.72
2	5.093	5.093	1.653	1.241	0.816	1.223	1.054	1.054	-98.61	3.41	15.79
4	5.204	5.205	1.671	1.265	0.848	1.248	1.168	1.168	-80.17	3.47	16.14
6	5.286	5.286	1.685	1.277	0.857	1.259	1.334	1.334	-47.65	3.51	16.40
8	5.453	5.453	1.693	1.284	0.864	1.267	2.907	2.907	298.79	3.53	16.94
10	5.514	5.514	1.716	1.303	0.878	1.285	1.803	1.803	43.81	3.58	17.13
12	5.569	5.569	1.757	1.333	0.897	1.315	1.885	1.885	58.63	3.66	17.29
14	5.651	5.651	1.768	1.343	0.906	1.324	1.959	1.959	70.28	3.69	17.55
16	6.017	6.017	1.787	1.361	0.922	1.342	2.055	2.055	67.86	3.74	18.73
18	6.159	6.159	1.832	1.394	0.943	1.375	2.111	2.111	71.26	3.83	19.18
20	6.271	6.271	1.86	1.419	0.961	1.399	2.166	2.166	76.29	3.90	19.53
22	6.357	6.357	1.884	1.439	0.980	1.419	2.215	2.215	81.62	3.95	19.79
24	6.581	6.581	1.914	1.463	0.997	1.442	2.231	2.231	70.55	4.02	20.51
26	6.702	6.702	2.590	1.970	1.331	1.942	2.727	2.727	173.76	5.41	20.53
28	6.985	6.985	2.743	2.099	1.435	2.070	2.845	2.845	181.54	5.77	21.37
30	7.065	7.065	2.812	2.156	1.480	2.126	2.949	2.949	199.71	5.92	21.59
32	7.178	7.178	3.021	2.277	1.513	2.246	3.072	3.072	219.96	6.26	21.87
34	7.347	7.347	3.150	2.382	1.592	2.349	3.073	3.073	208.64	6.54	22.35

TABLE-4
OBSERVED AND CALCULATED P AND T_λ, (λ = 2, 4, 6) cm^{-2} AT 303 K AND IN VARIOUS TIME INTERVALS FOR THE COMPLEX Pr(III):Leu:Mg(II)

Time	$^3H_4 \rightarrow {}^3P_2$		$^3H_4 \rightarrow {}^3P_1$		$^3H_4 \rightarrow {}^3P_0$		$^3H_4 \rightarrow {}^1D_2$		T_2	T_4	T_6
	P_{obs}	P_{cal}	P_{obs}	P_{cal}	P_{obs}	P_{cal}	P_{obs}	P_{cal}			
0	5.724	5.724	2.197	1.595	0.980	1.573	1.286	1.286	-88.52	4.38	17.61
2	5.741	5.741	2.289	1.680	1.057	1.657	1.360	1.360	-73.02	4.62	17.59
4	5.778	5.778	2.466	1.788	1.094	1.763	1.413	1.413	-63.75	4.91	17.64
6	5.938	5.938	2.577	1.887	1.181	1.861	1.679	1.679	-14.07	5.18	18.09
8	6.033	6.033	2.613	1.937	1.243	1.910	1.908	1.908	31.59	5.32	18.36
10	6.160	6.161	2.648	1.969	1.273	1.942	1.921	1.921	25.95	5.41	18.76
12	6.274	6.274	2.726	2.012	1.280	1.984	2.257	2.257	94.93	5.53	19.10
14	6.302	6.302	2.777	2.056	1.317	2.028	2.292	2.292	100.84	5.65	19.16
16	6.495	6.495	3.073	2.215	1.339	2.185	2.371	2.371	105.59	6.09	19.68
18	6.777	6.777	3.427	2.415	1.384	2.381	2.434	2.434	100.69	6.63	20.46
20	7.119	7.119	3.591	2.535	1.459	2.500	2.496	2.496	92.03	6.97	21.49
22	7.178	7.178	3.676	2.593	1.489	2.557	2.580	2.580	107.02	7.12	21.64
24	7.255	7.255	3.738	2.636	1.513	2.599	2.625	2.625	112.09	7.24	21.86
26	7.290	7.290	3.781	2.706	1.608	2.668	2.692	2.692	124.74	7.43	21.92
28	7.349	7.349	3.847	2.762	1.653	2.724	2.747	2.747	133.25	7.59	22.08
30	7.422	7.422	3.871	2.813	1.731	2.774	2.804	2.804	141.22	7.73	22.28
32	7.471	7.471	3.907	2.860	1.788	2.821	2.841	2.841	146.08	7.86	22.41
34	7.573	7.573	3.9831	2.919	1.830	2.879	2.888	2.888	150.07	8.02	22.69

transitions, the pseudo-hypersensitive $^3H_4 \rightarrow {}^3P_2$ transition exhibited the greatest sensitivity toward complex formation. The T_4 and T_6 parameters showed pronounced increases with reaction time and temperature, consistent with progressive formation of the Pr(III):Leu(II) complex.

The variation of observed oscillator strength (P_{obs}) with time for the $^3H_4 \rightarrow {}^3P_2$ transition at different temperatures is shown in Fig. 7. Rate constants were obtained from the slopes of the corresponding plots and are summarized in Table-7. The rate constant increased with temperature, following the order 313 K > 308 K > 303 K > 298 K, in accordance with Arrhenius behaviour. The increase in the frequency factor (A) with temperature is consistent with a higher probability of effective molecular collisions. The relatively low activation energy (E_a) confirmed that the complexation process proceeds with a comparatively small energetic barrier.

The plot of log k *versus* $(1/T) \times 10^3$ (Fig. 8) was used to determine the thermodynamic parameters ΔH^o, ΔS^o and ΔG^o, with the calculated values. The positive ΔH^o value indicates that complex formation is endothermic, whereas the negative ΔG^o value indicates that the process is thermodynamically spontaneous under the investigated conditions. The positive ΔS^o value points to an increase in the disorder of the system during coordination and supports an entropy-favoured complexation process (Table-8). The kinetic and thermodynamic parameters obtained from the 4*f*-4*f* absorption spectra provide

TABLE-5
OBSERVED AND CALCULATED P AND T_λ, (λ = 2, 4, 6) cm^{-2} AT 308 K AND IN VARIOUS TIME INTERVALS FOR THE COMPLEX Pr(III):Leu:Mg(II)

Time	$^3H_4 \rightarrow {}^3P_2$		$^3H_4 \rightarrow {}^3P_1$		$^3H_4 \rightarrow {}^3P_0$		$^3H_4 \rightarrow {}^1D_2$		T_2	T_4	T_6
	P_{obs}	P_{cal}	P_{obs}	P_{cal}	P_{obs}	P_{cal}	P_{obs}	P_{cal}			
0	6.191	6.190	1.703	1.367	1.017	1.348	0.854	0.854	-216.4	3.75	19.30
2	6.315	6.315	1.830	1.453	1.061	1.432	1.371	1.372	-107.3	3.99	19.65
4	6.415	6.415	1.912	1.498	1.069	1.477	1.519	1.519	-80.44	4.11	19.94
6	6.524	6.524	2.180	1.678	1.161	1.655	1.573	1.573	-75.99	4.61	20.17
8	6.612	6.612	2.461	1.846	1.213	1.820	2.034	2.034	22.40	5.07	20.33
10	6.649	6.649	2.587	1.923	1.242	1.897	2.091	2.091	32.84	5.28	20.40
12	7.022	7.021	2.635	1.957	1.261	1.929	2.154	2.154	22.67	5.37	21.59
14	7.118	7.118	2.878	2.098	1.301	2.069	2.303	2.303	49.51	5.76	21.81
16	7.118	7.118	2.878	2.098	1.300	2.069	2.303	2.303	49.51	5.76	21.81
18	7.290	7.290	3.005	2.190	1.357	2.160	2.443	2.443	69.85	6.02	22.30
20	7.362	7.362	3.045	2.221	1.378	2.190	2.526	2.526	83.97	6.10	22.52
22	7.431	7.431	3.085	2.245	1.385	2.214	2.568	2.568	88.82	6.17	22.73
24	7.459	7.459	3.212	2.320	1.408	2.287	2.641	2.641	103.23	6.37	22.76
26	7.532	7.532	3.329	2.387	1.425	2.354	2.696	2.696	110.86	6.56	22.95
28	8.088	8.088	3.331	2.396	1.441	2.363	2.771	2.771	91.34	6.58	24.77
30	8.344	8.344	3.336	2.408	1.461	2.375	2.817	2.817	84.94	6.62	25.60
32	8.356	8.356	3.341	2.417	1.473	2.383	2.854	2.854	92.55	6.64	25.63
34	8.386	8.386	3.348	2.431	1.493	2.397	2.909	2.909	103.13	6.68	25.72

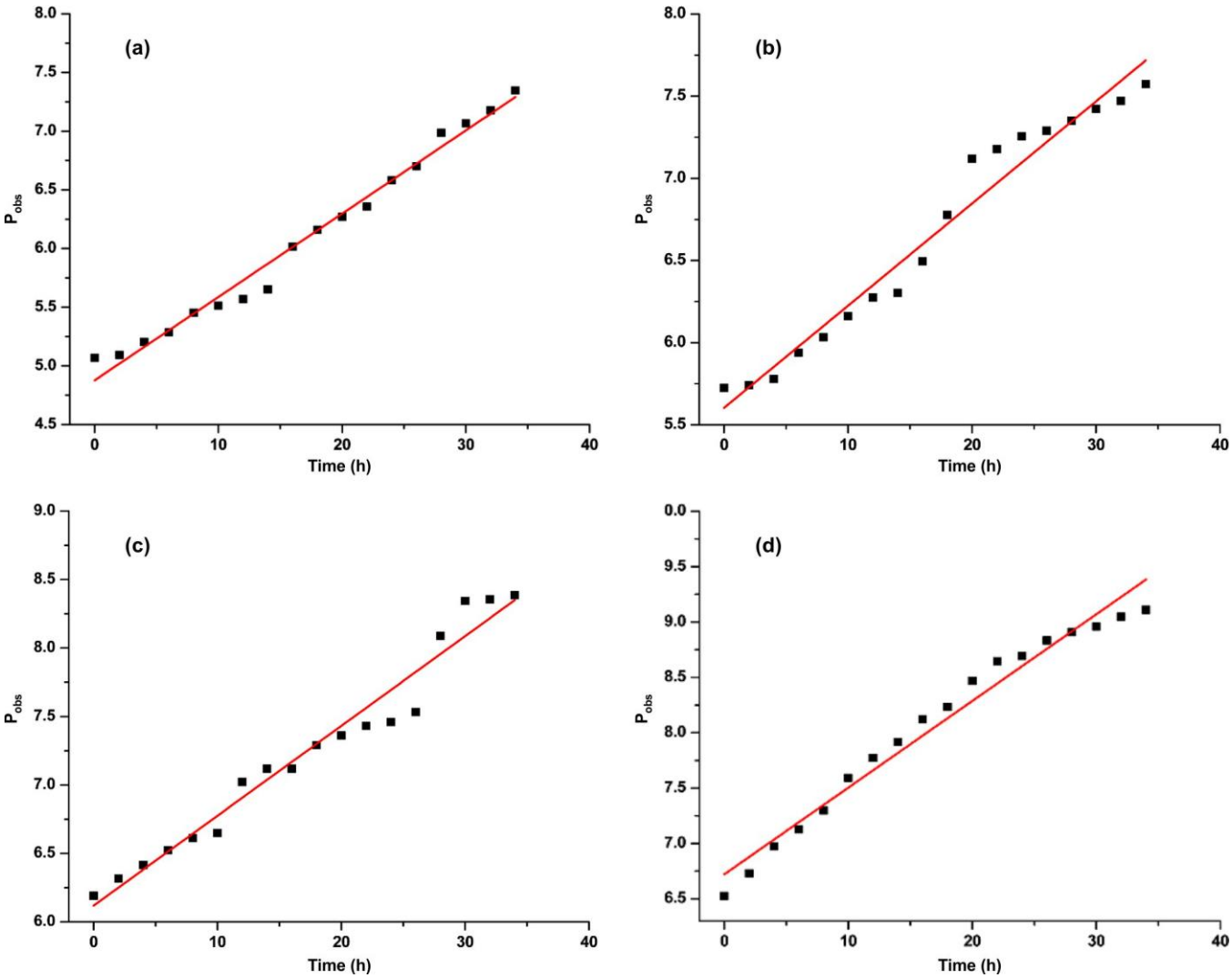

Fig. 7. P_{obs} *vs*. time (h) at different temperatures: (a) 298 K, (b) 303 K, (c) 308 K, (d) 313 K for the $^3H_4 \rightarrow {}^3P_2$ transition of Pr(III):Leu:Mg(II)

TABLE-6
OBSERVED AND CALCULATED P AND T_λ, (λ = 2, 4, 6) cm^{-2} AT 313 K AND IN VARIOUS TIME INTERVALS FOR THE COMPLEX Pr(III):Leu:Mg(II)

Time	$^3H_4 \rightarrow {}^3P_2$		$^3H_4 \rightarrow {}^3P_1$		$^3H_4 \rightarrow {}^3P_0$		$^3H_4 \rightarrow {}^1D_2$		T_2	T_4	T_6
	P_{obs}	P_{cal}	P_{obs}	P_{cal}	P_{obs}	P_{cal}	P_{obs}	P_{cal}			
0	6.525	6.525	1.780	1.302	0.811	1.283	1.236	1.236	-151.30	3.58	20.45
2	6.730	6.730	1.998	1.467	0.922	1.445	1.529	1.529	-98.90	4.03	21.01
4	6.974	6.974	2.264	1.623	0.966	1.599	1.810	1.810	-51.57	4.46	21.69
6	7.127	7.127	2.507	1.782	1.041	1.755	2.066	2.066	-3.96	4.89	22.07
8	7.297	7.297	2.530	1.823	1.101	1.796	2.253	2.253	27.35	5.01	22.61
10	7.591	7.591	2.647	1.945	1.224	1.916	2.434	2.434	48.82	5.34	23.48
12	7.772	7.772	2.880	2.088	1.277	2.057	2.619	2.619	78.38	5.74	23.96
14	7.914	7.914	3.001	2.162	1.303	2.130	2.812	2.812	112.73	5.94	24.38
16	8.121	8.121	3.080	2.219	1.338	2.186	2.957	2.957	132.05	6.10	25.02
18	8.232	8.232	3.193	2.324	1.434	2.290	3.137	3.137	165.17	6.39	25.31
20	8.467	8.467	3.269	2.377	1.463	2.342	3.343	3.343	196.47	6.53	26.04
22	8.643	8.643	3.337	2.426	1.492	2.390	3.385	3.385	194.38	6.67	26.58
24	8.692	8.692	3.390	2.480	1.547	2.443	3.576	3.576	234.29	6.81	26.70
26	8.832	8.832	3.437	2.522	1.583	2.485	3.653	3.653	242.37	6.93	27.13
28	8.908	8.908	3.463	2.552	1.617	2.514	3.727	3.727	254.21	7.01	27.35
30	8.959	8.959	3.507	2.589	1.646	2.550	3.794	3.794	266.04	7.11	27.49
32	9.046	9.046	3.644	2.668	1.666	2.628	3.844	3.844	271.29	7.33	27.72
34	9.109	9.109	3.663	2.686	1.684	2.646	3.897	3.897	279.16	7.38	27.91

TABLE-7
RATE CONSTANTS AND ACTIVATION ENERGY FOR Pr(III):Leu:Mg(II) COMPLEX AT VARIOUS TEMPERATURES

Temperature (K)	$1/T \times 10^3$ K^{-1}	Rate constant (k) (mol L^{-1} h^{-1})	Rate constant (k) (mol L^{-1} h^{-1}) × 10^{-6}	log k	Pre-exponential factor (A)	Activation energy ΔE_a (kJ/mol)
298	3.35	0.00463	16.67	1.22	4.87	0.0162
303	3.30	0.0539	19.40	1.29	5.60	
308	3.24	0.00591	21.27	1.33	6.12	
313	3.19	0.00648	23.33	1.36	6.72	

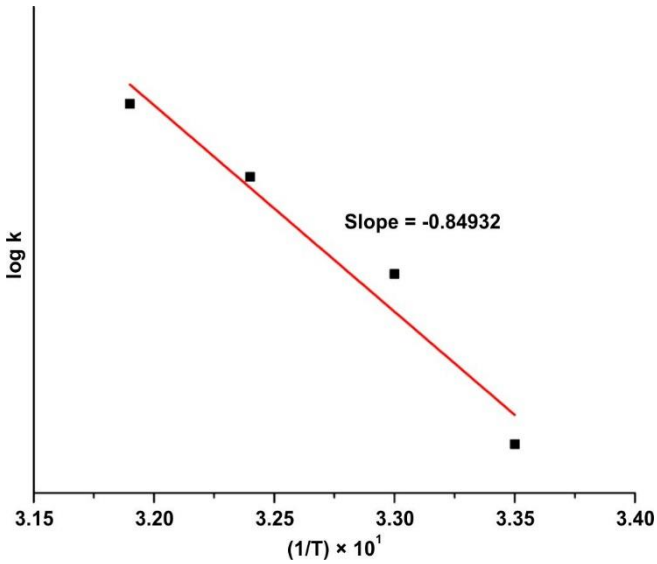

Fig. 8. log k *vs.* (1/T) × 10^3 for Pr(III):Leu:Mg(II) complex

useful information on the rate and energetics of Pr(III): Leu(II) complex formation.

Conclusion

The formation of the inner-sphere complexation during the interaction of Pr^{3+}, L-leucine and Mg^{2+} was indicated by the marked variations with the data of P and T_λ. Significant changes in the data of T_4 and T_6 imply that the symmetry of the complex formed might be altered. The rise of $b^{1/2}$ values and consistent decline in ξ_{4f}, E^k and F_k values could point to a possible interaction between the metal ion and the ligand. Addition of L-leucine to Pr^{3+} resulted in increased intensities of the 4*f*-4*f* absorption bands, accompanied by bathochromic shifts, confirmed the interaction between the metal ion and ligand. The decrease in β values points to a possible reduction in the Pr^{3+}–ligand bond distance. Changes in the intensity of the Pr^{3+} 4*f*-4*f* transitions upon addition of L-leucine and Mg^{2+} indicate changes in the coordination environment of the metal ion. Among the four solvents examined, DMF provided the most favourable medium for complex formation. The intensity parameters obtained at different reaction times and temperatures showed an increase in the rate of complex formation with increasing temperature, following Arrhenius behaviour. The

TABLE-8
RATE CONSTANTS AND THERMODYNAMIC PARAMETERS FOR Pr(III):Leu:Mg(II) COMPLEX AT VARIOUS TEMPERATURES

Temp. (K)	Rate constant (k) (mol L^{-1} h^{-1}) × 10^{-6}	ΔH^o (kJ mol^{-1})	ΔG^o (kJ mol^{-1})	ΔS^o (kJ mol^{-1})
298	1.22	0.0162	-6.96	0.039
303	1.29		-7.48	0.040
308	1.33		-7.84	0.041
313	1.36		-8.15	0.042

low activation energy (E_a) indicates that the complexation proceeds with a small energy barrier. The positive ΔH^o value confirms the endothermic nature of the complexation process, while the negative ΔG^o value indicates that the reaction is spontaneous and thermodynamically favourable in solution. The positive ΔS^o value, together with $T\Delta S^o > \Delta H^o$, which indicates that the Pr(III):Leu(II) complexation is predominantly entropy-driven. The temperature dependence of the frequency factor (A) further supports the relationship between molecular collision frequency and the rate of complex formation.

ACKNOWLEDGEMENTS

One of the authors, Zevivonü Thakro, is grateful to UGC, India for financial support in the form of Non-NET. The authors acknowledge the Department of Chemistry, Nagaland University, for providing the necessary facilities.

CONFLICT OF INTEREST

The authors declare that there is no conflict of interests regarding the publication of this article.

DECLARATION OF AI-ASSISTED TECHNOLOGIES

During the preparation of this manuscript, the authors used an AI-assisted tool(s) to improve the language and no data, results or scientific conclusions were generated by AI. All analyses, interpretations and conclusions are the authors' own. The authors reviewed and edited the content and take full responsibility for the published work.

REFERENCES

1. A.K. Pathak, D. Paudyal, Y. Mudryk and V.K. Pecharsky, *Phys. Rev. B*, **96**, 064412 (2017); https://doi.org/10.1103/PhysRevB.96.064412
2. K. Niu, F. Yang, T. Gaudin, H. Ma and W. Fang, *Inorg. Chem.*, **60**, 9552 (2021); https://doi.org/10.1021/acs.inorgchem.1c00657
3. P. Soni, G. Pagare and S.P. Sanyal, *J. Phys. Chem. Solids*, **71**, 1491 (2010); https://doi.org/10.1016/j.jpcs.2010.07.014
4. C. Chen and H. Li, *Z. Anorg. Allg. Chem.*, **645**, 888 (2019); https://doi.org/10.1002/zaac.201900009
5. K. Bernot, C. Daiguebonne, G. Calvez, Y. Suffren and O. Guillou, *Acc. Chem. Res.*, **54**, 427 (2021); https://doi.org/10.1021/acs.accounts.0c00684
6. J.C.G. Bünzli, *J. Coord. Chem.*, **67**, 3706 (2014); https://doi.org/10.1080/00958972.2014.957201
7. Y. Yang, X. Hu, Z. Yang and W. Huang, *Adv. Funct. Mater.*, **35**, 2412970 (2025); https://doi.org/10.1002/adfm.202412970
8. N. Bendangsenla, T. Moaienla, T. David Singh, C. Sumitra, N. Rajmuhon Singh, M. Indira Devi, *Spectrochim. Acta A Mol. Biomol. Spectrosc.*, **103**, 160 (2013); https://doi.org/10.1016/j.saa.2012.11.011
9. T.D. Singh, C. Sumitra, N. Yaiphaba, H.D. Devi, M.I. Devi and N.R. Singh, *Spectrochim. Acta A Mol. Biomol. Spectrosc.*, **61**, 1219 (2005); https://doi.org/10.1016/j.saa.2004.06.044
10. C. Berthomieu, M. Martin, J. Aupiais, T. Barré, L. Daronnat, J. Pansier, N. Brémond, D. Lemaire, A. Thawari, M. Levier, L. Berthon and S. Sauge-Merle, *Eur. J. Inorg. Chem.*, **29**, e202500468 (2026); https://doi.org/10.1002/ejic.202500468
11. G. Lanza, Z. Varga, M. Kolonits and M. Hargittai, *J. Chem. Phys.*, **128**, 074301 (2008); https://doi.org/10.1063/1.2828537
12. J.M. Han, S.J. Jeong, M.C. Park, G. Kim, N.H. Kwon, H.K. Kim, S.H. Ha, S.H. Ryu and S. Kim, *Cell*, **149**, 410 (2012); https://doi.org/10.1016/j.cell.2012.02.044
13. J.A.B. Pedroso, T.T. Zampieri and J. Donato Jr., *Nutrients*, **7**, 3914 (2015); https://doi.org/10.3390/nu7053914
14. L. Fu, A. Bruckbauer, F. Li, Q. Cao, X. Cui, R. Wu, H. Shi, M.B. Zemel and B. Xue, *Metabolism*, **64**, 845 (2015); https://doi.org/10.1016/j.metabol.2015.03.007
15. C.J. Lynch and S.H. Adams, *Nat. Rev. Endocrinol.*, **10**, 723 (2014); https://doi.org/10.1038/nrendo.2014.171
16. N.E. Cummings, E.M. Williams, I. Kasza, E.N. Konon, M.D. Schaid, B.A. Schmidt, C. Poudel, D.S. Sherman, D. Yu, S.I. Arriola Apelo, S.E. Cottrell, G. Geiger, M.E. Barnes, J.A. Wisinski, R.J. Fenske, K.A. Matkowskyj, M.E. Kimple, C.M. Alexander, M.J. Merrins and D.W. Lamming, *J. Physiol.*, **596**, 623 (2018); https://doi.org/10.1113/JP275075
17. B. Dhanalakshmi, B. Padmadevi and G. Suresh, *J. Mater. Sci. Mater. Electron.*, **37**, 513 (2026); https://doi.org/10.1007/s10854-026-16922-9
18. N. Ranjana Devi, B. Huidrom and N. Rajmuhon Singh, *Spectrochim. Acta A Mol. Biomol. Spectrosc.*, **96**, 370 (2012); https://doi.org/10.1016/j.saa.2012.05.038
19. Z. Thakro, M.T. Ao, C. Imsong, J. Sanchu, M. Ziekhrü and M.I. Devi, *Eur. Phys. J. Plus*, **137**, 608 (2022); https://doi.org/10.1140/epjp/s13360-022-02765-w
20. U. Gröber, J. Schmidt and K. Kisters, *Nutrients*, **7**, 8199 (2015); https://doi.org/10.3390/nu7095388
21. M. Pelczyńska, M. Moszak and P. Bogdański, *Nutrients*, **17**, 1714 (2022); https://doi.org/10.3390/nu14091714
22. G.K. Schwalfenberg and S.J. Genuis, *Scientifica*, **2017**, 4179326 (2017); https://doi.org/10.1155/2017/4179326
23. K.K. Gangu, S. Maddila, S.N. Maddila and S.B. Jonnalagadda, *Molecules*, **21**, 1281 (2016); https://doi.org/10.3390/molecules21101281
24. M.F. Bush, J. Oomens, R.J. Saykally and E.R. Williams, *J. Am. Chem. Soc.*, **130**, 6463 (2008); https://doi.org/10.1021/ja711343q
25. F. Costanzo, R.G. Della Valle and V. Barone, *J. Phys. Chem. B*, **109**, 23016 (2005); https://doi.org/10.1021/jp055271g
26. M. Remko, D. Fitz, R. Broer and B.M. Rode, *J. Mol. Model.*, **17**, 3117 (2011); https://doi.org/10.1007/s00894-011-1000-0
27. A.L. Sobolewski, D. Shemesh and W. Domcke, *J. Phys. Chem. A*, **113**, 542 (2009); https://doi.org/10.1021/jp8091754
28. J.C.G. Bünzli and C. Piguet, *Chem. Rev.*, **102**, 1897 (2002); https://doi.org/10.1021/cr010299j
29. A.M. Măciucă, A.C. Munteanu and V. Uivarosi, *Molecules*, **25**, 1347 (2020); https://doi.org/10.3390/molecules25061347
30. C. Sumitra, T.D. Singh, M.I. Devi and N.R. Singh, *J. Alloys Compd.*, **451**, 365 (2008); https://doi.org/10.1016/j.jallcom.2007.04.153
31. G.S. Ofelt, *J. Chem. Phys.*, **37**, 511 (1962); https://doi.org/10.1063/1.1701366
32. B.R. Judd, *Phys. Rev.*, **127**, 750 (1962); https://doi.org/10.1103/PhysRev.127.750
33. M. Luo, B. Chen, X. Li, J. Zhang, S. Xu, X. Zhang, Y. Cao, J. Sun, Y. Zhang, X. Wang, Y. Zhang, D. Gao and L. Wang, *Phys. Chem. Chem. Phys.*, **22**, 25177 (2020); https://doi.org/10.1039/D0CP04379F
34. K. Binnemans and C. Görller-Walrand, *Chem. Rev.*, **102**, 2303 (2002); https://doi.org/10.1021/cr010287y
35. J.H. Van Vleck, *J. Phys. Chem.*, **41**, 67(1937); https://doi.org/10.1021/j150379a006
36. A.A. Kornienko, A.A. Kaminskii and E.B. Dunina, *Phys. Status Solidi (b)*, **157**, 267 (1990); https://doi.org/10.1002/pssb.2221570127

37. Z. Thakro, J. Sanchu, C. Imsong and M. Indira Devi, *Chem. Phys. Impact*, **4**, 100078 (2022); https://doi.org/10.1016/j.chphi.2022.100078
38. Y. Tian, B. Chen, R. Hua, J. Sun, L. Cheng, H. Zhong, X. Li, J. Zhang, Y. Zheng, T. Yu, L. Huang and H. Yu, *J. Appl. Phys*., **109**, 053511 (2011); https://doi.org/10.1063/1.3551584
39. J.L. Ryan and C.K. Jørgensen, *J. Phys. Chem.*, **70**, 2845 (1966); https://doi.org/10.1021/j100881a021
40. M.S.A. Munna, T. Hossain, M.S. Islam, O.T. Mefford, H. Ahmad and M.M. Rahman, *RSC Adv.*, **16**, 11793 (2026); https://doi.org/10.1039/D5RA09579D
41. Y.F. Zhao, H. Bin Chu, F. Bai, D.Q. Gao, H.X. Zhang, Y.S. Zhou, X.Y. Wei, M.N. Shan, H.Y. Li and Y.L. Zhao, *J. Organomet. Chem.*, **716**, 167 (2012); https://doi.org/10.1016/j.jorganchem.2012.06.031
42. L. Sorace, C. Benelli and D. Gatteschi, *Chem. Soc. Rev.*, **40**, 3092 (2011); https://doi.org/10.1039/c0cs00185f
43. S. Chizo, V. Sapu, S. Singha and M.I. Devi, *J. Solution Chem.*, **55**, 1123 (2026); https://doi.org/10.1007/s10953-025-01545-1
44. N. Bendangsenla, T. Moaienla, T. David Singh, C. Sumitra, N. Rajmuhon Singh and M. Indira Devi, *Spectrochim. Acta A Mol. Biomol. Spectrosc.*, **103**, 160 (2013); https://doi.org/10.1016/j.saa.2012.11.011
45. J.B. Gruber, G.W. Burdick, S. Chandra and D.K. Sardar, *J. Appl. Phys.*, **108**, 023109 (2010); https://doi.org/10.1063/1.3465615
46. R.D. Peacock, The intensities of lanthanide f ↔ f transitions, In: Rare Earths, Structure and Bonding, Rare Earths, Springer, Berlin, Heidelberg, vol 22, pp. 83-122 (1975).
47. W.T. Carnall, P.R. Fields and K. Rajnak, *J. Chem. Phys.*, **49**, 4447 (1968); https://doi.org/10.1063/1.1669895
48. C. Victory Devi and N. Rajmuhon Singh, *Arab. J. Chem.*, **10**, S2124 (2017); https://doi.org/10.1016/j.arabjc.2013.07.044
49. A.A. Khan, H.A. Hussain and K. Iftikhar, *Spectrochim. Acta A Mol. Biomol. Spectrosc.*, **60**, 2087 (2004); https://doi.org/10.1016/j.saa.2003.10.042
50. T. Moaienla, T.D. Singh, N.R. Singh and M.I. Devi, *Spectrochim. Acta A Mol. Biomol. Spectrosc.*, **74**, 434 (2009); https://doi.org/10.1016/j.saa.2009.06.039
51. N. Bendangsenla, T. Moainla, J. Sanchu and M.I. Devi, *J. Mater. Sci. Chem. Eng.*, **6**, 169 (2018); https://doi.org/10.4236/msce.2018.67018
52. M. Ziekhrü, Z. Thakro, C. Imsong, J. Sanchu and M.I. Devi, *Polyhedron*, **200**, 115099 (2021); https://doi.org/10.1016/j.poly.2021.115099
53. N. Bendangsenla, M.I. Devi, T. Moaienla and R. Zatsu, *J. Adv. Chem. Sci.*, **4**, 556 (2018); https://doi.org/10.30799/jacs.182.18040201
54. Z.A. Taha, A.K. Hijazi and W.M. Al Momani, *J. Mol. Struct.*, **1220**, 128712 (2020); https://doi.org/10.1016/j.molstruc.2020.128712